Applied Physics Letters

Offcut-related step-flow and growth rate enhancement during (100) β-Ga_2O_3 homoepitaxy by metal-exchange catalyzed molecular beam epitaxy (MEXCAT-MBE)

Cite as: Appl. Phys. Lett. **117**, 222105 (2020); https://doi.org/10.1063/5.0031300
Submitted: 30 September 2020 . Accepted: 14 November 2020 . Published Online: 01 December 2020

Piero Mazzolini, Andreas Falkenstein, Zbigniew Galazka, Manfred Martin, and Oliver Bierwagen

Applied Physics Letters ARTICLE scitation.org/journal/apl

Offcut-related step-flow and growth rate enhancement during (100) β-Ga_2O_3 homoepitaxy by metal-exchange catalyzed molecular beam epitaxy (MEXCAT-MBE)

Cite as: Appl. Phys. Lett. **117**, 222105 (2020); doi: 10.1063/5.0031300
Submitted: 30 September 2020 · Accepted: 14 November 2020 ·
Published Online: 1 December 2020

Piero Mazzolini,[1,a),b)] Andreas Falkenstein,[2] Zbigniew Galazka,[3] Manfred Martin,[2] and Oliver Bierwagen[1,b)]

AFFILIATIONS

[1]Paul-Drude-Institut für Festkörperelektronik, Leibniz-Institut im Forschungsverbund Berlin e.V., Hausvogteiplatz 5-7, 10117 Berlin, Germany
[2]Institute of Physical Chemistry, RWTH Aachen University, D-52056 Aachen, Germany
[3]Leibniz-Institut für Kristallzüchtung, Max-Born-Str. 2, 12489 Berlin, Germany

Note: This paper is part of the Special Topic on Ultrawide Bandgap Semiconductors.
[a)]**Present address:** Department of Mathematical, Physical and Computer Sciences, University of Parma, Viale delle Scienze 7/A, 43124 Parma, Italy.
[b)]**Authors to whom correspondence should be addressed:** piero.mazzolini@unipr.it and bierwagen@pdi-berlin.de

ABSTRACT

Homoepitaxial β-Ga_2O_3 layers grown via molecular beam epitaxy (MBE) have exhibited prohibitively low growth rates on (100) oriented substrates in the past. In this work, we investigate the possibility to employ indium-assisted metal exchange catalyzed (MEXCAT) MBE to overcome this limit. We demonstrate that the fine tuning of the MEXCAT growth parameters and the choice of a proper substrate offcut allow for the deposition of thin films with high structural quality via the step-flow growth mechanism at relatively high growth rates for β-Ga_2O_3 homoepitaxy (i.e., around 1.5 nm/min, $\approx$ 45% incorporation of the incoming Ga flux), making MBE growth in this orientation feasible. Moreover, through the employment of the four investigated different (100) substrate offcuts along the $[00\bar{1}]$ direction (i.e., 0°, 2°, 4°, and 6°), we give experimental evidence on the fundamental role of the $(\bar{2}01)$ step edges as nucleation sites in the growth of (100)-oriented Ga_2O_3 films by MBE.

β-Ga_2O_3 plays an important role in new generation power electronic devices.[1] A great advantage for this ultra-wide bandgap oxide is the possibility to produce bulk material from the melt,[2] enabling the homoepitaxial growth of high-quality β-Ga_2O_3 thin films. Among the different growth techniques, molecular beam epitaxy (MBE)[3–5] and metalorganic chemical vapor deposition or metalorganic vapor phase epitaxy (MOCVD or MOVPE)[6–8] have so far emerged for providing the highest quality β-Ga_2O_3 homoepitaxial layers. Nonetheless, the chosen substrate orientation for homoepitaxial deposition of β-Ga_2O_3 can pose two major challenges: (1) the possible formation of structural defects and (2) the presence of different growth rates (GRs). The first point is related to the low symmetry of the monoclinic cell of β-Ga_2O_3, which, due to the possible double positioning of Ga atoms and island coalescence during the growth process, eventually results in the creation of twins in both the (100)[9,10] and $(\bar{2}01)$[4] homoepitaxial growth, eventually affecting the electrical properties of the layers.[11] Nonetheless, for MOVPE (100) homoepitaxy, it has been possible to overcome this problem with the choice of an appropriate substrate offcut so as to allow the step flow growth of the layers in the presence of $(\bar{2}01)$ steps.[7,8] The second challenge in β-Ga_2O_3 homoepitaxy is the different GR recorded as a function of different substrate orientations. This mostly affects the MBE growth technique[3,12] and is mostly related to the peculiar growth kinetics of Ga_2O_3 during MBE growth, which involves the intermediate formation of the Ga_2O volatile suboxide;[13–15] the tendency of Ga_2O to desorb from the sample surface before its further oxidation in Ga_2O_3 is dependent on the growth surface itself. This has so far limited the investigation of MBE-grown β-Ga_2O_3 homoepitaxial layers to the (010) growth plane, i.e., the one with the highest surface free energy out of the most experimentally used ones [(100), (010), (001), and $(\bar{2}01)$].[7,16] For the (010) plane, GRs as high

as ≈ 2.2 nm/min[3] and 3.2 nm/min[17] have been reported for ozone and plasma-assisted MBE, respectively. The other β-Ga_2O_3 surfaces and especially the most stable (100) cleavage plane[7,16] generally suffer from lower GRs in MBE (e.g., ≈ 0.15 nm/min[3] and ≈ 0.3 nm/min[18] for ozone and plasma-assisted MBE, respectively). Differently, for MOVPE, negligible substrate orientation dependencies have been reported with respect to the GR, probably because of different Ga_2O_3 growth kinetics compared to the MBE process;[8] in particular, for (100) MOVPE homoepitaxy, high-quality layers were deposited with GRs between 1.6 nm/min and 4.3 nm/min on substrates offcut toward $[00\bar{1}]$.[8]

The (100) β-Ga_2O_3 growth surface is potentially very interesting because of the possibility to obtain step-flow growth, resulting in smooth layers with high structural quality[7,8] [similar to what has been recently demonstrated in (010) homoepitaxy with proper substrate offcuts[19]]. Unfortunately, the low GRs of the MBE process so far have practically limited the homoepitaxial synthesis in the (100) orientation solely to the MOVPE technique. Nonetheless, it has been recently demonstrated that the addition of an In[20] or Sn[21] metal flux can allow one to widen the growth window of Ga_2O_3 in MBE by the metal-exchange catalysis (MEXCAT) mechanism.[15] Indium-mediated MEXCAT has been recently successfully applied in the MBE homoepitaxial growth of β-Ga_2O_3 layers over different orientations,[4,5,19,22] as well as β-$(Al,Ga)_2O_3$ layers on β-Ga_2O_3(010) substrates.[23] In particular, with MEXCAT-MBE, it has been possible to demonstrate that the use of (100) substrates with a 6° offcut results in homoepitaxial layers with a high structural quality comparable to the one obtained in MOVPE growth.[4,7] Nonetheless, the GR has been found to be still a function of the β-Ga_2O_3 growth surface,[4] proving that the MEXCAT-MBE process can mitigate but not fully eliminate the partial loss of the incoming Ga flux from highly stable surfaces like the (100) one. In particular, the GR obtained for high-quality MEXCAT-MBE β-Ga_2O_3 homoepitaxial layers on 6°-off (100) substrates was around 0.27 nm/min (i.e., corresponding to less than 10% incorporation of the incoming Ga flux), the lowest one with respect to the other tested β-Ga_2O_3 orientations [i.e., (010), (001), and $(\bar{2}01)$]. As a comparison, the same Ga flux can be fully incorporated in (010)-oriented MEXCAT-MBE homoepitaxy (i.e., 3.3 nm/min),[19] while Mauze *et al.*[5] using a similar experimental approach were able to obtain GRs as high as ≈ 5 nm/min in the same substrate orientation, proving that the GR can be maximized by properly increasing the provided metal and oxygen fluxes.

In the present work, throughout the optimization of the MEXCAT-MBE deposition process and the understanding of the role of the offcut angle in (100) homoepitaxy, we demonstrate step-flow growth rates (GRs) of ≈ 1.5 nm/min (≈ 45% incorporation of Ga flux) comparable to the ones obtained by the MOVPE growth technique on offcut (100) substrates.

Mg-doped (100) β-Ga_2O_3 substrates with $[00\bar{1}]$-oriented offcuts of 0°, 2°, 4°, and 6° prepared from bulk crystals obtained by the Czochralski method[24,25] were employed. The substrate preparation prior to the deposition is explained in our previous work.[4] The depositions were performed in an MBE chamber with an O-plasma source run at a power of 300 W for a fixed deposition time of 30 minutes. The substrate temperatures were monitored using an optical pyrometer. The beam equivalent pressure (BEP) of Ga was fixed to $BEP_{Ga} \approx 1.2 \times 10^{-7}$ mbar (particle flux $\Phi_{Ga} = 2.2\,nm^{-2}\,s^{-1}$), corresponding to a GR ≈ 3.3 nm/min at full Ga incorporation (thickness ≈ 100 nm). The In flux for the MEXCAT process is set to be $\Phi_{In} = 1/3\ \Phi_{Ga}$ ($BEP_{In} \approx 5.2 \times 10^{-8}$ mbar). Both the metal fluxes were maintained constant for all the growth, while the oxygen flow and the growth temperatures were varied among 0.75 standard cubic centimeters per minute (sccm) and 1 sccm, and $T_g = 700$–$800\,°C$. An $(Al_xGa_{1-x})_2O_3$ marker layer at the substrate-layer interface was deposited (deposition time = 80 s) in almost all the growth runs; the related details are reported in a previous work.[4] The (100) β-Ga_2O_3 substrates with different offcuts were co-loaded so that they are subjected to the same deposition conditions in a single growth run. The growth rate was calculated from the growth time and layer thickness determined using the In signal from time-of-flight secondary ion mass spectrometry (ToF-SIMS IV from IONTOF GmbH) depth profiling (interference microscope WYKO NT1100 from Veeco Instruments Inc., with an error of about 1% to 3% in the layer thickness) and/or by x-ray diffraction (XRD) fringe interspace in the vicinity of the β-Ga_2O_3 400 reflex (out-of-plane 2θ-ω scans PANalytical X'Pert Pro MRD using Cu Kα radiation). The In content from SIMS was obtained using a concentration calibration.[4] The sample surface was investigated by atomic force microscopy (AFM Bruker Dimension Edge) in PeakForce tapping mode.

In Table I we report a summary of the collected results. In agreement with our previous investigation of the growth kinetics and thermodynamics of Ga_2O_3 by MBE and MEXCAT-MBE, a lower T_g or higher O flux not only increases GR[4,13–15,20,22] but also increases the tendency of indium incorporation during MEXCAT-MBE.[4] More importantly, for all the tested growth conditions, the GR is generally higher for larger offcuts, as also shown in Fig. 1(b). Moreover, comparing the lowest tested T_g runs (i.e., 740 °C and 700 °C), it is interesting to highlight that both the depositions on 0°- and 2°-off substrates show similar (740 °C) or equal (700 °C) GRs, while higher offcuts in both cases result in a clear GR increment [Table I and Fig. 1(b)]. In the following, we try to give a physical explanation for this result: as reported by Schewski *et al.*[7,26] and schematically illustrated in Fig. 1(a), an offcut along the $[00\bar{1}]$ direction in (100) β-Ga_2O_3 substrates results in the formation of (100) terraces with different widths—i.e., 16.9 nm, 8.5 nm, and 5.6 nm for 2°-, 4°-, and 6°-off, respectively; 0.59 nm steps are formed among the terraces, leaving exposed $(\bar{2}01)$-oriented surfaces at the step edges[7] [Fig. 1(a)].

The MBE growth on the (100) surface is complicated because of its high stability (i.e., low surface free energy, leading to increased desorption during growth),[7,16] resulting in limited GRs;[3,18] even if mitigated, this is also true in the case of MEXCAT-MBE as proved by the data reported in Table I for 0°-off substrates. Furthermore, we have recently demonstrated[4] that the homoepitaxial growth on $(\bar{2}01)$-oriented substrates via MEXCAT-MBE allows for layer depositions at higher T_g (and/or lower O fluxes) with respect to the (100) orientation—i.e., because of the higher surface energy of the $(\bar{2}01)$ with respect to the (100) one. As an example in Table I, we give the reference growth rate measured on $(\bar{2}01)$-oriented β-Ga_2O_3 substrates (nominally 0°-offcut)[4] for the highest T_g/lowest O flux investigated in the present study, which is significantly higher (2.2 nm/min) than that on the 0°-offcut (100) substrate (0.1 nm/min).

Generally, growth takes place by a sequence of adsorption, diffusion, and nucleation competing with the desorption of the surface diffusing species.[27] In the particular case of oxides like Ga_2O_3 and In_2O_3[14] (both potentially involved at different stages of the

TABLE I. Growth rates of (100)-oriented β-Ga_2O_3 layers deposited in four different growth runs via MEXCAT-MBE (different offcuts co-loaded). A growth rate for $(\bar{2}01)$ homoepitaxy and a non-catalyzed growth are also reported for comparison (data taken from Ref. 4). In the growth rate column, we report in parentheses the experimental methods used to determine the thickness. The In content obtained from SIMS is reported for samples to be ≥ 10 nm.

T_g (°C)	O flux (sccm)	Offcut (°)	Growth rate (nm/min)		In content (cm^{-3})
800	0.75	0 on $(\bar{2}01)$ (Ref. 4)	2.2	(SIMS)	1×10^{19}
		0	0.1	(SIMS)	
		2	0.17	(SIMS)	
		6 (from Ref. 4)	0.33	(SIMS)	2×10^{18}
		6 (from Ref. 4) Non-catalyzed growth	0	(SIMS)	
800	1	2	0.17	(SIMS)	
		4	0.33	(XRD)	
		6	0.47	(XRD + SIMS)	2×10^{18}
740	0.75	0	0.17	(SIMS)	
		2	0.2	(SIMS)	
		4	0.37	(XRD)	
		6	0.8	(XRD + SIMS)	$3\text{-}7 \times 10^{18}$
700	0.75	0	0.33	(SIMS)	2×10^{19}
		2	0.33	(XRD + SIMS)	1.1×10^{19}
		4	0.67	(XRD)	
		6	1.5	(XRD + SIMS)	$1.6\text{-}1.9 \times 10^{19}$

MEXCAT-MBE deposition process[15,20]), their peculiar growth kinetics involves the intermediate formation of their respective volatile suboxide molecules (Ga_2O and In_2O), which we consider the relevant, diffusing, and desorbing species. We propose that a possible explanation of our experimental findings [Table I, Fig. 1(b)] can be found in (i) the $(\bar{2}01)$-oriented step edges acting as nucleation sites for the surface diffusing species during growth [see Fig. 1(c)] and (ii) the influence of the growth condition on the diffusion length and desorption of the adsorbed species on the (100) surface. In order to reach the $(\bar{2}01)$ edges, the adsorbed species must diffuse on the (100) terraces along the [001] direction, and thus, only species adsorbed within a diffusion length from the step edge can contribute to growth. Consequently, for the tested growth conditions (T_g and O fluxes) of this work, the diffusion length on the (100) surface along the [001] direction should be limited to less than the associated terrace length of the 4° offcut substrate, i.e., ≈ 8.5 nm, to explain the growth-rate increase upon increasing the offcut to 6°, for example. Larger offcuts result in shorter terrace lengths, and thus, species adsorbed on a larger area fraction of the terraces are within a diffusion length from the step edges and can contribute to growth. Consequently, the GR increases with the increasing offcut [Fig. 1(b)]. (For the films grown at 745 and 700 °C, the relative increase in GR due to increasing offcut from 4° to 6° is, however,

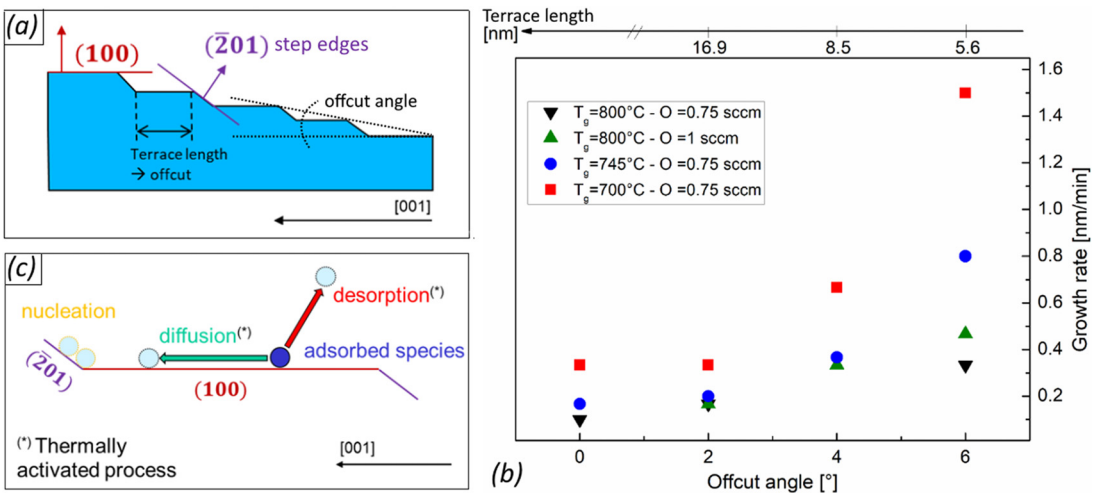

FIG. 1. (a) Sketch representing a cross-sectional view of (100) offcut substrates; (b) offcut and associated terrace length as a function of the obtained growth rate for different synthesis conditions (see Table I); (c) schematic representation of the growth process on (100) offcut substrates via MBE.

larger than the associated relative increase in step density, calling for clarification by more detailed modeling such as the Kinetic Monte Carlo study of Ref. 27). The surface diffusion length λ_S can be expressed as a function of the diffusion coefficient on the surface D_S and the mean diffusion time τ_S as $\lambda_S = \sqrt{D_S \tau_S}$.[28] Importantly, τ_S is the time between adsorption and desorption of the diffusing species from the (100) terrace, i.e., the inverse of the desorption rate. Since diffusion and desorption are thermally activated processes, λ_S can also be expressed as a function of the barrier energy for the desorption rate and the surface diffusion coefficient E_{des} and E_{diff}, respectively: $\lambda_S \propto e^{\frac{E_{des}-E_{diff}}{2kT_g}}$, where k is the Boltzmann constant. The decreasing GR with increasing T_g [Fig. 1(b)] at all chosen offcut angles indicates a decreasing λ_S, suggesting that $E_{des} > E_{diff}$ in our case, i.e., a stronger increase in the desorption rate than the increase in the surface diffusion coefficient.

The fact that we do not observe a saturation of GR with the increasing miscut angle suggests that values larger than 6° further increases GR. Besides higher miscut angles (that may become impractical at some point), a further decrease in the desorption rate (increase in τ_S) can also lead to higher growth rates. This, in turn, may be achieved by further decreasing the growth temperature and simultaneous optimization of the In, Ga, and O fluxes to sustain a step flow growth and prevent excessive In incorporation. A recent report on high temperature low pressure chemical vapor deposition (HT-LPCVD) of $(\bar{2}01)$ β-Ga_2O_3 layers on offcut c-plane sapphire substrates also found an increasing GR with the increasing offcut angle,[29] whereas MOVPE (100) homoepitaxy did not highlight any GR dependence for the same offcuts investigated in the present work.[8] These HT-LPCVD and MOVPE results are difficult to compare among each other due to different synthesis techniques, deposition conditions, and layer orientations; they, however, seem to indicate non-negligible and negligible desorption from the terraces, respectively.

The explanation presented here is also supported by the collected AFM micrographs obtained for the samples deposited at the lowest T_g (700 °C, Fig. 2). In such deposition conditions, we report the growth of an ≈ 10 nm thick film in both 0°- and 2°-off substrates [XRD trace in Fig. 2(b) (green) is in agreement with results obtained from SIMS (not shown)]. Nonetheless, in both samples, it is possible to identify the presence of islands elongated along the [010] direction [Fig. 2(a), 0° and 2°]. Such islands have already been highlighted in homoepitaxial layers grown by MOVPE[26] and MBE[10] on exactly oriented (100) substrates, and their elongation could be a sign of a lower diffusion length of the adsorbed species on the (100) surface along the [001] direction than in the [010] one. The coalescence of these islands usually results in the formation of twins.[9] The same could potentially happen for also the layers deposited on top of the 2°-offcut substrate [Fig. 2(a)] in our MEXCAT-MBE growth due to island nucleation on the terraces of the 2°-off substrate [visible as the interruption of the regular step-terrace lines along the [010] direction in Fig. 2(a)] instead of nucleation at the $(\bar{2}01)$ step edges. Differently, the surface

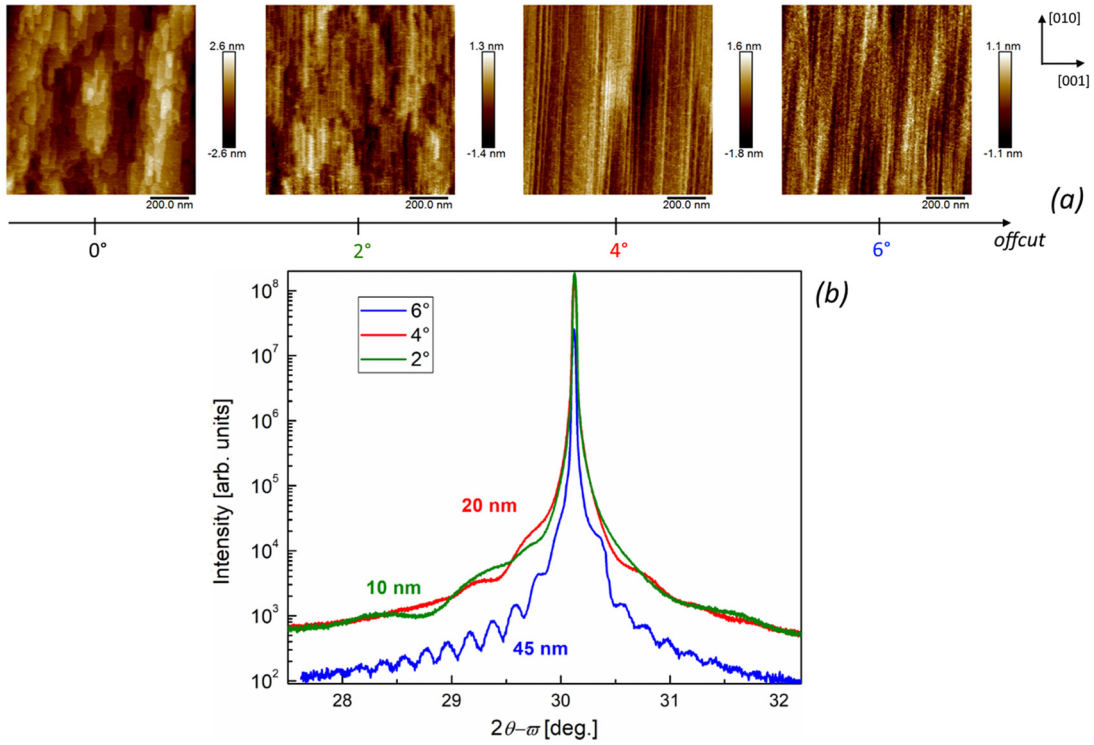

FIG. 2. (a) AFM micrographs of (100) β-Ga_2O_3 homoepitaxial layers deposited via MEXCAT-MBE at $T_g = 700$ °C with O flux = 0.75 sccm on different offcut substrates [red squares in Fig. 1(b)]. In (b) the corresponding XRD scans of the 400 reflection for the 2°, 4°, and 6°-off samples are reported with relative thicknesses from respective thickness fringes.

morphology of the 4° and 6°-off samples [Fig. 2(a)], despite larger film thicknesses with respect to the 0° and 2°-off ones [Fig. 2(b)], suggests a step-flow or (partially) a step-bunched growth, resulting in a more regular and smooth layer surface.

We now focus on the 6°-off samples deposited under the 4 different tested growth conditions (Table I). Their AFM images [Fig. 3(a)] show the effect of the substrate temperature and (just for one sample deposited at 800 °C) of the O flux on the surface morphology. Under all the deposition conditions for the 6°-off layers, no structural defects are expected, as already evidenced by the TEM investigation of the sample deposited at 800 °C with O flux = 0.75 sccm presented in Ref. 4. Nonetheless, despite the limited root mean square roughness (rms = 0.3 nm) of this layer [Fig. 3(a)], step bunching can be highlighted (see the TEM image of this layer in Figure 5 of Ref. 4). An increase in the O flux while maintaining the very same T_g resulted in an increased step bunching mechanism (rms = 1.3 nm) probably related to an increased diffusion length by suppressed desorption[14] through the increased oxygen species on the surface. On the other hand, decreasing the T_g down to 740 °C while maintaining the O flux at 0.75 sccm drastically reduced the step bunching, going toward a step-flow growth mechanism (rms = 0.19 nm). Nonetheless, the thickest layer deposited at the lowest T_g (700 °C, O flux = 0.75 sccm) shows an intermediate roughness (rms = 0.32 nm); the reasons are still not fully understood.

With these samples deposited with In-mediated MEXCAT-MBE, both T_g and O flux employed should decisively affect the concentration of incorporated In inside the deposited layer: a lower T_g and/or a higher O flux during the deposition process was shown to be connected to a larger amount of In inside the sample.[4] As visible from Fig. 3(b) (values reported in Table I), this trend is confirmed for the investigated T_g, while for different O fluxes (0.75–1 sccm), the measured In concentration is basically unchanged; this is probably related to the low layer thickness and the presence of an In peak at the substrate-film interface (Fig. 3), which is already highlighted for β-Ga_2O_3 MEXCAT-MBE homoepitaxy.[4] The deposition conditions that resulted in the highest growth rate of 1.5 nm/min—i.e., T_g = 700 °C, O flux = 0.75 sccm—also result in the highest In incorporation ($\approx 1.6–1.9 \times 10^{19}$ cm^{-3}). Nevertheless, as already discussed in a previous work,[4] such concentrations should not affect the electrical properties of the layer as In is isovalent with Ga and such low concentrations would only lead to a negligible bandgap decrease. Moreover, the data reported in Table I on the series of samples deposited on the different offcut substrates under the same synthesis conditions (i.e., T_g = 700 °C, O flux = 0.75 sccm—0°, 2°, and 6°) consistently show that the amount of incorporated In is not affected by the offcut itself, but just by the deposition conditions. Finally, we highlight that the current understanding of the MEXCAT-MBE deposition technique for β-Ga_2O_3 homoepitaxy[4,5] suggests that a low amount of incorporated catalyst element (i.e., indium) can be just obtained with growth parameters that result in very little (or no) growth rate in a standard MBE deposition (e.g., non-catalyzed MBE at T_g = 800 °C and O flux = 0.75 sccm on the 6° substrate resulted in no layer growth, see Table I).

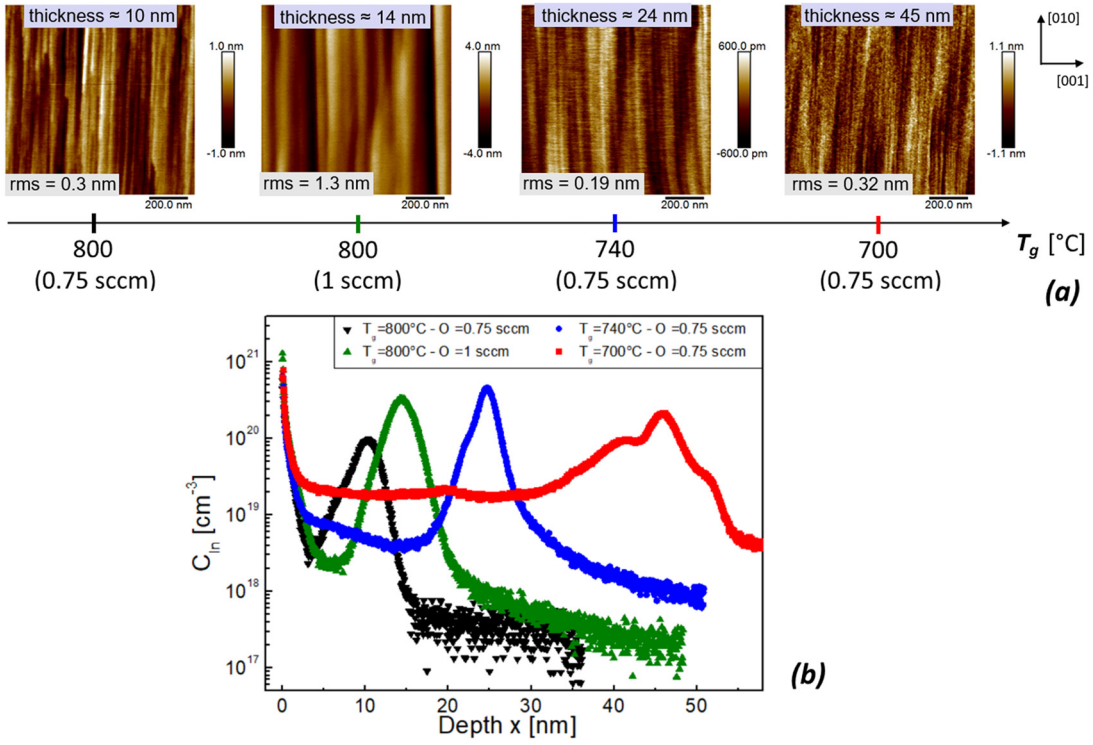

FIG. 3. (a) AFM micrographs of (100) β-Ga_2O_3 homoepitaxial layers deposited via MEXCAT-MBE at different T_g values or O fluxes for the same 6° substrate offcut. (b) Indium concentration C_{In} depth profiles for the same samples extracted by ToF-SIMS. The film thickness is equated with the depth of the In-accumulation peak at the layer-substrate interface. The AFM image and the SIMS profile of the sample deposited at 800 °C with 0.75 sccm flux have already been presented in Ref. 4.

In conclusion, we have shown how In-mediated MEXCAT MBE can be considered as a viable technique for the deposition of high-quality (100) β-Ga_2O_3 homoepitaxial layers. In particular, we have demonstrated step-flow growth on substrates offcut toward the $[00\bar{1}]$ direction at growth rates comparable to the ones obtained by the MOVPE technique in this substrate orientation. Different from MOVPE results,[8] during MEXCAT-MBE, an increasing growth rate with the increasing offcut angle was found and related to almost exclusive layer nucleation on the $(\bar{2}01)$-oriented step edges due to their higher surface free energy (and, thus, lower propensity for desorption) than that of the (100)-oriented terraces. Regarding the obtained absolute growth rate value of 1.5 nm/min, the authors remind us that this could be scaled by further increasing the offcut angle, decreasing the growth temperature, or—as already demonstrated for the (010) orientation[5]—by scaling up the Ga and O fluxes. We believe that our result, together with the deep understanding of the underlying physical processes, could represent an important step further for the realization of β-Ga_2O_3-based power electronic heterostructured and/or homostructured devices by MBE on (100)-oriented substrates.

The authors express their gratitude to Jens Herfort and Thomas Teubner for critical reading of this manuscript, as well as Hans-Peter Schönherr, Carsten Stemmler, and Katrin Morgenroth for technical MBE support. The authors would also like to thank Jutta Schwarzkopf and Daniel Pfützenreuter for scientific discussion and experimental help related to the MBE depositions. This work was performed in the framework of GraFOx, a Leibniz-Science Campus partially funded by the Leibniz Association.

DATA AVAILABILITY

The data that support the findings of this study are available from the corresponding author upon reasonable request.

REFERENCES

[1]S. J. Pearton, J. Yang, P. H. Cary, F. Ren, J. Kim, M. J. Tadjer, and M. A. Mastro, Appl. Phys. Rev. **5**, 011301 (2018).
[2]Z. Galazka, Semicond. Sci. Technol. **33**, 113001 (2018).
[3]K. Sasaki, A. Kuramata, T. Masui, E. G. Víllora, K. Shimamura, and S. Yamakoshi, Appl. Phys. Express **5**, 035502 (2012).
[4]P. Mazzolini, A. Falkenstein, C. Wouters, R. Schewski, T. Markurt, Z. Galazka, M. Martin, M. Albrecht, and O. Bierwagen, APL Mater. **8**, 011107 (2020).
[5]A. Mauze, Y. Zhang, T. Itoh, F. Wu, and J. S. Speck, APL Mater. **8**, 021104 (2020).
[6]Y. Zhang, F. Alema, A. Mauze, O. S. Koksaldi, R. Miller, A. Osinsky, and J. S. Speck, APL Mater. **7**, 022506 (2019).
[7]R. Schewski, K. Lion, A. Fiedler, C. Wouters, A. Popp, S. V. Levchenko, T. Schulz, M. Schmidbauer, S. Bin Anooz, R. Grüneberg, Z. Galazka, G. Wagner, K. Irmscher, M. Scheffler, C. Draxl, and M. Albrecht, APL Mater. **7**, 022515 (2019).
[8]S. Bin Anooz, R. Grüneberg, C. Wouters, R. Schewski, M. Albrecht, A. Fiedler, K. Irmscher, Z. Galazka, W. Miller, G. Wagner, J. Schwarzkopf, and A. Popp, Appl. Phys. Lett. **116**, 182106 (2020).
[9]G. Wagner, M. Baldini, D. Gogova, M. Schmidbauer, R. Schewski, M. Albrecht, Z. Galazka, D. Klimm, and R. Fornari, Phys. Status Solidi A **211**, 27 (2014).
[10]Z. Cheng, M. Hanke, Z. Galazka, and A. Trampert, Nanotechnology **29**, 395705 (2018).
[11]A. Fiedler, R. Schewski, M. Baldini, Z. Galazka, G. Wagner, M. Albrecht, and K. Irmscher, J. Appl. Phys. **122**, 165701 (2017).
[12]Y. Oshima, E. Ahmadi, S. Kaun, F. Wu, and J. S. Speck, Semicond. Sci. Technol. **33**, 015013 (2018).
[13]P. Vogt and O. Bierwagen, Appl. Phys. Lett. **108**, 072101 (2016).
[14]P. Vogt and O. Bierwagen, Phys. Rev. Mater. **2**, 120401(R) (2018).
[15]O. Bierwagen, P. Vogt, and P. Mazzolini, in *Gallium Oxide Materials Properties, Crystal Growth, and Devices*, edited by M. Higashiwaki and S. Fujita (Springer International Publishing, Cham, 2020), pp. 95–121.
[16]V. M. Bermudez, Chem. Phys. **323**, 193 (2006).
[17]E. Ahmadi, O. S. Koksaldi, S. W. Kaun, Y. Oshima, D. B. Short, U. K. Mishra, and J. S. Speck, Appl. Phys. Express **10**, 041102 (2017).
[18]M.-Y. Tsai, O. Bierwagen, M. E. White, and J. S. Speck, J. Vac. Sci. Technol., A **28**, 354 (2010).
[19]P. Mazzolini and O. Bierwagen, J. Phys. D: Appl. Phys. **53**, 354003 (2020).
[20]P. Vogt, O. Brandt, H. Riechert, J. Lähnemann, and O. Bierwagen, Phys. Rev. Lett. **119**, 196001 (2017).
[21]M. Kracht, A. Karg, J. Schörmann, M. Weinhold, D. Zink, F. Michel, M. Rohnke, M. Schowalter, B. Gerken, A. Rosenauer, P. J. Klar, J. Janek, and M. Eickhoff, Phys. Rev. Appl. **8**, 054002 (2017).
[22]P. Mazzolini, P. Vogt, R. Schewski, C. Wouters, M. Albrecht, and O. Bierwagen, APL Mater. **7**, 022511 (2019).
[23]P. Vogt, A. Mauze, F. Wu, B. Bonef, and J. S. Speck, Appl. Phys. Express **11**, 115503 (2018).
[24]Z. Galazka, R. Uecker, D. Klimm, K. Irmscher, M. Naumann, M. Pietsch, A. Kwasniewski, R. Bertram, S. Ganschow, and M. Bickermann, ECS J. Solid State Sci. Technol. **6**, Q3007 (2017).
[25]Z. Galazka, K. Irmscher, R. Uecker, R. Bertram, M. Pietsch, A. Kwasniewski, M. Naumann, T. Schulz, R. Schewski, D. Klimm, and M. Bickermann, J. Cryst. Growth **404**, 184 (2014).
[26]R. Schewski, M. Baldini, K. Irmscher, A. Fiedler, T. Markurt, B. Neuschulz, T. Remmele, T. Schulz, G. Wagner, Z. Galazka, and M. Albrecht, J. Appl. Phys. **120**, 225308 (2016).
[27]W. Miller, D. Meiling, R. Schewski, A. Popp, S. B. Anooz, and M. Albrecht, Phys. Rev. Res. **2**, 033170 (2020).
[28]I. Bryan, Z. Bryan, S. Mita, A. Rice, J. Tweedie, R. Collazo, and Z. Sitar, J. Cryst. Growth **438**, 81 (2016).
[29]Y. Zhang, Z. Feng, M. R. Karim, and H. Zhao, J. Vac. Sci. Technol., A **38**, 050806 (2020).